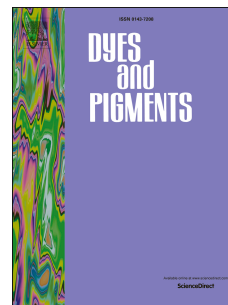


Accepted Manuscript

Phenanthro[9,10-*d*]imidazole based new host materials for efficient red phosphorescent OLEDs

Daiva Tavgeniene, Gintare Krucaite, Urte Baranauskyte, Jian-Zhi Wu, Hong-Yu Su, Chih-Wei Huang, Chih-Hao Chang, Saulius Grigalevicius



PII: S0143-7208(16)30674-X

DOI: [10.1016/j.dyepig.2016.11.003](https://doi.org/10.1016/j.dyepig.2016.11.003)

Reference: DYPI 5571

To appear in: *Dyes and Pigments*

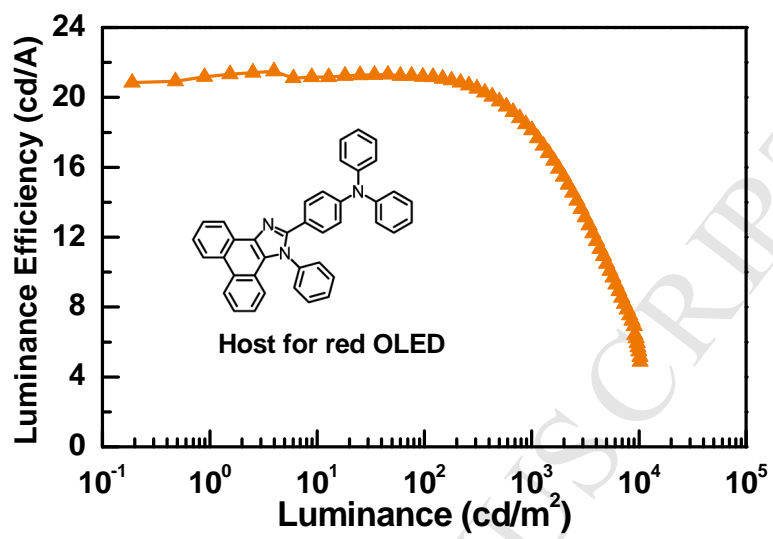
Received Date: 7 September 2016

Revised Date: 2 November 2016

Accepted Date: 3 November 2016

Please cite this article as: Tavgeniene D, Krucaite G, Baranauskyte U, Wu J-Z, Su H-Y, Huang C-W, Chang C-H, Grigalevicius S, Phenanthro[9,10-*d*]imidazole based new host materials for efficient red phosphorescent OLEDs, *Dyes and Pigments* (2016), doi: 10.1016/j.dyepig.2016.11.003.

This is a PDF file of an unedited manuscript that has been accepted for publication. As a service to our customers we are providing this early version of the manuscript. The manuscript will undergo copyediting, typesetting, and review of the resulting proof before it is published in its final form. Please note that during the production process errors may be discovered which could affect the content, and all legal disclaimers that apply to the journal pertain.



Phenanthro[9,10-*d*]imidazole based New Host Materials for Efficient Red Phosphorescent OLEDs

Daiva Tavgeniene¹, Gintare Krucaite¹, Urte Baranauskyte¹, Jian-Zhi Wu², Hong-Yu Su², Chih-Wei Huang², Chih-Hao Chang^{2,*}, Saulius Grigalevicius^{1,*}

¹Department of Polymer Chemistry and Technology, Kaunas University of Technology, Radvilenu plentas 19, LT50254, Kaunas, Lithuania

²Department of Photonics Engineering, Yuan Ze University, Chung-Li, Taiwan 32003

* Corresponding authors:

chc@saturn.yzu.edu.tw (C.H. Chang), saulius.grigalevicius@ktu.lt (S. Grigalevicius)

Abstract

We report on the synthesis and characterization of a new series of bipolar phenanthro[9,10-*d*]imidazole based compounds. The derivatives are highly thermally stable materials as demonstrated by thermogravimetric analysis. Electron photoemission spectra of thin layers of the materials show ionization potentials in the range of 5.1-5.4 eV. Spectroscopic properties of the phenanthro[9,10-*d*]imidazole based derivatives were determined by absorption and photoluminescence measurements. All the developed materials were used as hosts in red phosphorescent organic light-emitting diodes and their properties were compared with commercially available host materials. Results indicate that a device with 2-[4-(*N,N*-diphenylamino)phenyl]-1-phenylphenanthro[9,10-*d*]imidazole exhibited superior performance with peak efficiency of 15.9% (21.5 cd/A and 29.9 lm/W) and very low turn on voltage of 2.8 V. Efficiency of the device is about 35-67% higher than those of devices containing commercial host materials.

Keywords: Phenanthro[9,10-*d*]imidazole, host material, ionization potential, phosphorescent, organic light-emitting diode.

Introduction

Applications of organic light-emitting devices (OLED) based displays are expanding rapidly due to their superior performance and flexibility as compared with liquid crystal displays. Phosphorescent OLEDs (PhOLEDs) have particularly attracted researchers because of their higher efficiencies compared with those of fluorescent OLED devices [¹]. In order to achieve the high efficiency, the triplet energy should be confined on the phosphorescent dopant without endothermic energy transfer to the host material. Multiple-layer configurations have been widely developed to enhance efficiency of blue and green phosphorescent PhOLEDs. Red phosphorescent materials with a lower triplet energy gap enable the simplification of the device architecture; however the lower gap of the phosphors usually induces serious carrier trapping, leading to higher operation voltages [²]. There are only several reports describing rather efficient red PhOLEDs [^{3, 4, 5}]. Accordingly, it is important to develop new host materials for realizing the red devices with high performance.

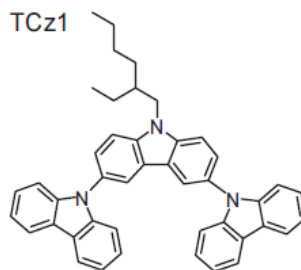
Carbazole and triphenylamine fragments possess several commendable properties, including chemical stability, convenient modification and large triplet energy etc. [^{6, 7, 8, 9, 10, 11}]. Consequently, many successful host or hole transport materials adopted carbazole or triphenylamine-containing designs. Our group synthesized the carbazole based material, 3,6-di(9-carbazolyl)-9-(2-ethylhexyl) carbazole (TCz1), which possesses structurally rigid moieties and a nonplanar molecular configuration, resulting in a morphologically-stable molecule with a wide triplet energy gap [¹²]. Sky blue PhOLEDs with a TCz1 host were demonstrated with efficiencies of up to 15 %, 31 cd/A, and 28 lm/W. We have also observed recently that carbazole-based bipolar derivatives are effective host materials for PhOLED devices [^{13, 14}]. A green dry-processed device showed a current efficiency of 61 cd/A and a power efficiency of 62.8 lm/W. In this paper, we

describe a series of new phenanthro[9,10-*d*]imidazole based derivatives for bipolar emitting host. The red PhOLEDs with 2-[4-(*N,N*-diphenylamino)phenyl]-1-phenylphenanthro[9,10-*d*]imidazole (**H2**) as host material exhibited superior performance with peak efficiency of 15.9% (21.5 cd/A and 29.9 lm/W) and very low turn-on voltage of 2.8 V.

Experimental

Materials

3,6-Di(9-carbazolyl)-9-(2-ethylhexyl) carbazole (TCz1) was prepared by the procedure described in literature [12].



9*H*-carbazole (**1**), triphenylamine (**4**), 1-bromohexane, acetone, potassium hydroxide (KOH), tetrabutylammonium hydrogensulfate (TBAHS), phosphorus oxychloride (POCl₃), dimethylformamide (DMF), chloroform, dichloromethane, aniline, acetic acid, ammonium acetate and 9,10-phenanthrenequinone were purchased from Aldrich and used as received.

9-Hexylcarbazole (**2**) was prepared by procedure described in the literature [15]. 3-Formyl-9-hexylcarbazole (**3**), 4-(diphenylamino)benzaldehyde (**5**) and 4,4'-diformyltriphenylamine (**6**) were obtained by a Vilsmeier reaction [16] using earlier described procedures [17, 18].

2-(9-Hexylcarbazolyl-3-yl)-1-phenylphenanthro[9,10-*d*]imidazole (**H1**). 3-Formyl-9-hexylcarbazole (**3**) (1.0 g, 3.58 mmol), 9,10-phenanthrenequinone (0.82 g, 3.94 mmol), ammonium acetate (1.11 g, 14.40 mmol) and aniline (1.67 g, 17.93 mmol) were stirred in acetic acid (15 mL) at 120 °C under nitrogen for 2 h. After thin layer chromatography (TLC) control the reaction mixture was cooled down to the room temperature and poured into ice water. The resulting residue

that had been formed was filtered off, washed with water and dissolved in chloroform. The solution was dried by Na_2SO_4 and the solvent was removed by evaporation. The product was purified by column chromatography with silica gel using chloroform/hexane (vol. ratio 2:3) as an eluent. Yellow crystals, 62% (1.2 g), mp 202 °C. IR data (KBr): 2925, 1714, 1599, 1495, 1454, 1417, 1381, 1353, 1238, 1142, 889, 816, 767, 748, 721 cm^{-1} . ^1H NMR δ_{H} (CDCl_3 , 500 MHz): 8.96 (d, 1H, $J = 8.0$ Hz, Ar), 8.78 (d, 1H, $J = 8.4$ Hz, Ar), 8.72 (d, 1H, $J = 8.0$ Hz, Ar), 8.25 (d, 1H, $J = 1.2$ Hz, Ar), 7.19 (d, 1H, $J = 8.0$ Hz, Ar), 7.82–7.72 (m, 2H, Ar), 7.73–7.55 (m, 6H, Ar), 7.56–7.17 (m, 7H, Ar), 4.25 (t, 2H, $J = 7.2$ Hz, NCH_2), 1.90–1.79 (m, 2H, NCH_2CH_2), 1.39–1.27 (m, 6H, $2 \times \text{NCH}_2\text{CH}_2\text{CH}_2\text{CH}_2\text{CH}_2$), 0.86 (t, 3H, $J = 6.8$ Hz, CH_3). ^{13}C NMR δ_{C} (CDCl_3 , 125 MHz): 151.74, 140.82, 138.69, 130.26, 129.32, 127.52, 127.45, 126.38, 126.05, 124.16, 123.10, 122.03, 120.90, 120.49, 119.34, 108.94, 108.56, 43.22, 31.55, 28.93, 26.94, 22.55, 14.02. HRMS found: $[\text{M}+\text{H}]^+$ 544.7236; molecular formula $\text{C}_{39}\text{H}_{33}\text{N}_3$ requires $[\text{M}+\text{H}]^+$ 544.7267. Elemental analysis for $\text{C}_{39}\text{H}_{33}\text{N}_3$ % Calc.: C 86.15, H 6.12, N 7.73; % Found: C 86.11, H 6.14, N 7.71.

2-[4-(*N,N*-diphenylamino)phenyl]-1-phenylphenanthro[9,10-*d*]imidazole (**H2**). 4-(Diphenylamino)benzaldehyde (**5**) (1.0 g, 3.66 mmol), 9,10-phenanthrenequinone (0.83 g, 3.99 mmol), ammonium acetate (1.13 g, 14.66 mmol) and aniline (1.70 g, 18.25 mmol) were stirred in acetic acid (20 ml) at 120 °C under nitrogen for 2 h. After TLC control the reaction mixture was cooled down to the room temperature and poured into ice water. The resulting residue that had been formed was filtered off, washed with water and dissolved in chloroform. The solution was dried by Na_2SO_4 and the solvent was removed by evaporation. The product was purified by column chromatography with silica gel using chloroform/hexane (vol. ratio 2:3) as an eluent. Yellow crystals, 64% (1.3 g), mp 285 °C. IR data (KBr): 1588, 1516, 1485, 1468, 1453, 1424, 1383, 1330, 1281, 1195, 1076, 1037, 966, 840, 747, 735, 720 cm^{-1} . ^1H NMR δ_{H} (CDCl_3 , 500 MHz): 8.87 (d, 1H, $J = 8.0$ Hz, Ar), 8.76 (d, 1H, $J = 8.4$ Hz, Ar), 8.69 (d, 1H, $J = 8.4$ Hz, Ar), 7.78–7.69 (m, 1H, Ar), 7.68–7.40 (m, 9H, Ar), 7.30–7.21 (m, 5H, Ar), 7.16–7.00 (m, 7H, Ar), 6.97–6.89 (m, 2H, Ar). ^{13}C

NMR δ_C (CDCl₃, 125 MHz): 150.63, 148.56, 147.15, 138.83, 130.23, 130.23, 129.93, 129.38, 129.22, 129.18, 128.29, 127.90, 127.34, 126.30, 125.69, 125.13, 124.84, 124.13, 123.60, 123.09, 122.94, 121.81, 120.78. HRMS found: [M+H]⁺ 538.6741; molecular formula C₃₉H₂₇N₃ requires [M+H]⁺ 538.6752. Elemental analysis for C₃₉H₂₇N₃ % Calc.: C 87.12, H 5.06, N 7.82; % Found: C 87.05, H 5.09, N 7.79.

Bis[4-(1-phenylphenanthro[9,10-*d*]imidazol-2-yl)phenyl]-*N*-phenylamine (**H3**). 4,4'-diformyltriphenylamine (**6**) (1g, 3.32 mmol), 9,10-phenanthrenequinone (1.52 g, 7.30 mmol), ammonium acetate (2.05 g, 26.6 mmol) and aniline (3.09 g, 33.18 mmol) were stirred in acetic acid (20 mL) at 120 °C under nitrogen for 3 h. After TLC control the reaction mixture was cooled down to the room temperature and poured into ice water. The residue that had been formed was filtered off, washed with water and dissolved in chloroform. The solution was dried by Na₂SO₄ and the solvent was removed by evaporation. The product was purified by column chromatography with silica gel using chloroform/hexane (vol. ratio 1:1) as an eluent. Yellow crystals, 44% (1.2 g), mp 361 °C. IR data (KBr): 1738, 1599, 1536, 1514, 1494, 1469, 1453, 1382, 1344, 1320, 1286, 1265, 1183, 1073, 1046, 957, 833, 759, 740, 723 cm⁻¹. ¹H NMR δ_H (CDCl₃, 500 MHz): 8.87 (d, 2H, *J* = 7.6 Hz, Ar), 8.77 (d, 2H, *J* = 8.0 Hz, Ar), 8.70 (d, 2H, *J* = 8.0 Hz, Ar), 7.78-7.71 (m, 2H, Ar), 7.69-7.60 (m, 7H, Ar), 7.58-7.44 (m, 9H, Ar), 7.31-7.23 (m, 6H, Ar), 7.19-7.12 (m, 2H, Ar), 7.11-7.04 (m, 3H, Ar), 6.99-6.93 (m, 4H, Ar). ¹³C NMR δ_C (CDCl₃, 125 MHz): 149.49, 146.69, 145.57, 137.84, 136.40, 129.23, 128.94, 128.72, 128.46, 128.21, 128.11, 127.26, 127.00, 126.28, 125.28, 124.61, 123.80, 123.10, 122.07, 121.82, 119.77. HRMS found: [M+H]⁺ 831.0147; molecular formula C₆₀H₃₉N₅ requires [M+H]⁺ 831.0136. Elemental analysis for C₆₀H₃₉N₅ % Calc.: C 87.05, H 4.74, N 8.44; % Found: C 87.01, H 4.77, N 8.41.

Thermal and photophysical characterization

Differential scanning calorimetry (DSC) measurements were carried out using a Bruker Reflex II thermos system. Thermogravimetric analysis (TGA) was performed on a Netzsch STA 409. The TGA and DSC curves were recorded in a nitrogen atmosphere at a heating rate of 10° C/min.

The absorption spectra were performed by using a UV-VIS Spectrophotometer (Shimadzu, UV-1650PC). The fluorescent and phosphorescent spectra of materials in CH₂Cl₂ were measured by using a Fluorolog III photoluminescence spectrometer (Horiba Jovin Yvon).

The electron photoemission method for measurement of ionization potentials (I_p) of the solid state layers of the studied compounds was exploited in air [19]. The vacuum deposited layers of the compounds onto commercial indium tin oxide (ITO) coated glass substrates were utilized as the samples for the electron photoemission measurements. The deep-UV deuterium light source ASBN-D130-CM, CM110 1/8m monochromator, and 6517B Keithley electrometer were used in the experimental setup, which was similar as previously described [20].

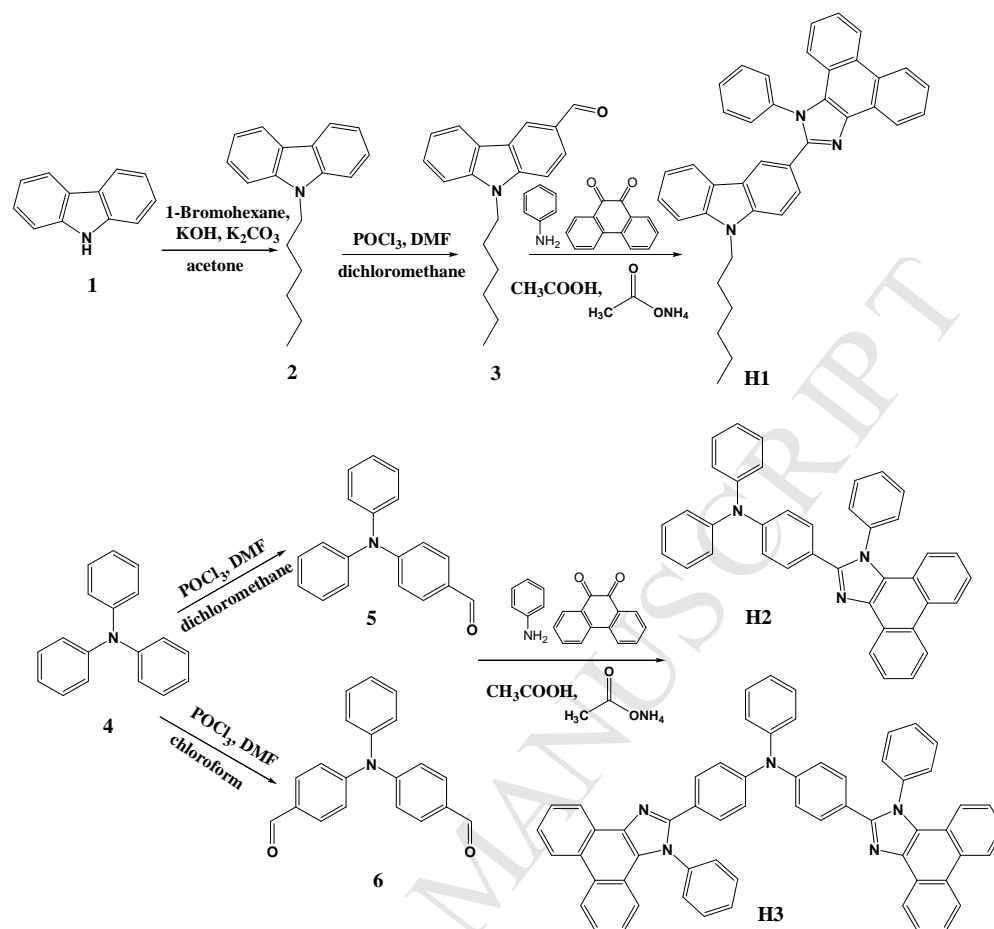
Device fabrication

Indium tin oxide (ITO)-coated glass and OLED materials were purchased from Nichem and Lumtec. The latter were subjected to temperature-gradient sublimation in a high vacuum before use. After a routine cleaning procedure, the ITO substrate was pretreated with UV-Ozone for 5 minutes. The organic and metal layers were deposited onto ITO-coated glass by thermal evaporation in a vacuum chamber with a base pressure of $< 10^{-6}$ Torr. Device fabrication was completed in a single cycle without breaking the vacuum. The deposition rates of the organic materials and aluminium were respectively kept at around 0.1 nm/s and 0.5 nm/s. The active area was defined by the shadow mask (2×2 mm²). Current density-voltage-luminance characterization was measured using a Keithley 238 current source-measure unit and a Keithley 6485 picoammeter equipped with a calibrated Si-photodiode. The electroluminescent spectra were recorded using an Ocean Optics spectrometer.

Results and Discussion

Synthesis and thermal properties of the materials.

The synthesis of 1-phenylphenanthro[9,10-*d*]imidazole based host materials (**H1-H3**) was carried out by a multi-step synthetic route as shown in Scheme 1. 9-Hexylcarbazole (**2**) was firstly synthesized by reaction of commercially available carbazole (**1**) with an excess 1-bromohexane under basic conditions in acetone. 3-Formyl-9-hexylcarbazole (**3**) was then prepared from the compound **2** by a Vilsmeier formylation procedure. 4-(Diphenylamino)benzaldehyde (**5**) and 4,4'-diformyltriphenylamine (**6**) were obtained from triphenylamine (**4**) by a Vilsmeier formylation procedure in chloroform or dichloromethane, respectively. The objective materials, i.e. 2-(9-hexylcarbazolyl-3-yl)-1-phenylphenanthro[9,10-*d*]imidazole (**H1**), 2-[4-(*N,N*-diphenylamino)phenyl]-1-phenylphenanthro[9,10-*d*]imidazole (**H2**) and bis[4-(1-phenylphenanthro[9,10-*d*]imidazol-2-yl)phenyl]-*N*-phenylamine (**H3**) were prepared by the reactions of the aldehydes **3**, **5** or **6** with excess of 9,10-phenanthrenequinone, aniline and ammonium acetate in acetic acid. The synthesized derivatives were all identified by mass spectrometry and ¹H NMR spectroscopy. The data were found to be in good agreement with the proposed structures. The materials were soluble in common organic solvents. Transparent thin films of these materials could be prepared by spin coating from solutions or by vacuum evaporation.

Scheme 1. Synthetic pathway of the materials **H1-H3**

The behaviour under heating of the objective materials **H1- H3** was studied by DSC and TGA under a nitrogen atmosphere. The data are summarized in Table 1 and presented in Figures 1 and 2. It was established that all of the objective compounds demonstrate high thermal stability. The mass loss of 5 % (T_{ID}) were at 386 °C for **H1**, at 414 °C for **H2** and at 448 °C for **H3**, as confirmed by TGA with a heating rate of 10° C/min. It could be observed that triphenylamine-based derivatives (**H2** and **H3**) demonstrate slightly higher thermal stability than that of 9-alkylcarbazole containing material **H1**.

All the compounds **H1- H3** were obtained as crystalline materials after synthesis as confirmed by DSC, however some of the materials could be easily converted to amorphous materials by cooling the melted samples. The derivative **H2** demonstrated very strong tendency to crystallization. DSC thermo-grams of **H2** are shown in Figure 1. When the crystalline sample was heated during the

experiment, an endothermic peak due to melting (T_m) was observed at 285 °C. When the melt sample was cooled down, its crystallization (T_{cr}) was observed at 223 °C to form the same crystals, which were obtained by crystallization from solution.

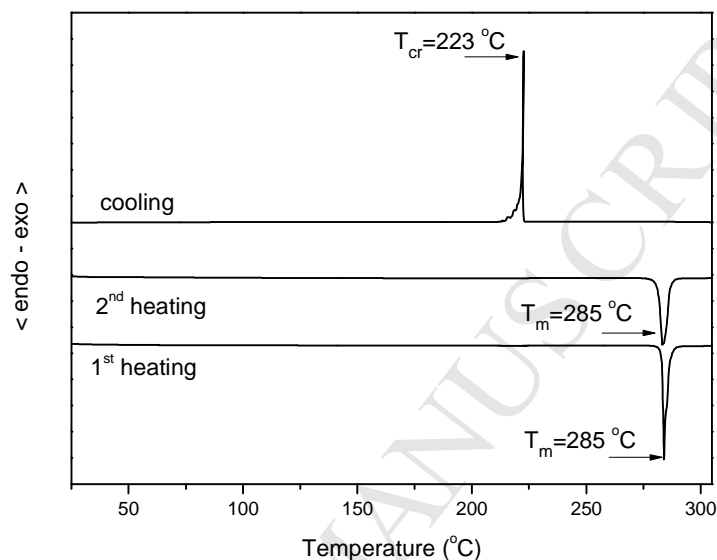


Figure 1. DSC curves of compound **H2**. Heating rate: 10 °C/min.

Compounds **H1** and **H3** demonstrated different behaviour during the DSC experiments. Thermograms of compound **H3** are shown in Figure 2 as an example. When a crystalline sample of **H3** was heated, melting was observed at 318 °C followed by fast crystallization at 321 °C to form new crystalline modification, which melted at 361 °C. When the molten sample was cooled down, it formed an amorphous material with high glass transition temperature (T_g) of 184 °C. The compound **H1** demonstrated an analogous behaviour during the DSC test. When its crystalline sample was heated during the experiment, melting was observed at 152 °C followed by recrystallization at 166 °C. The new crystalline modification melted then at 204 °C. When the melt sample was cooled down, it formed an amorphous material with glass transition temperature of 52 °C.

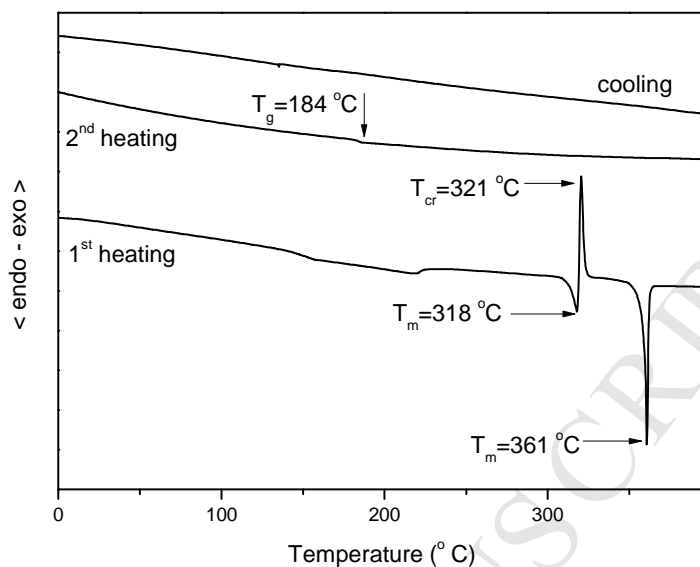


Figure 2. DSC curves of compound **H3**. Heating rate: $10\text{ }^\circ\text{C}/\text{min}$.

Photoemission, absorption and photoluminescence spectra.

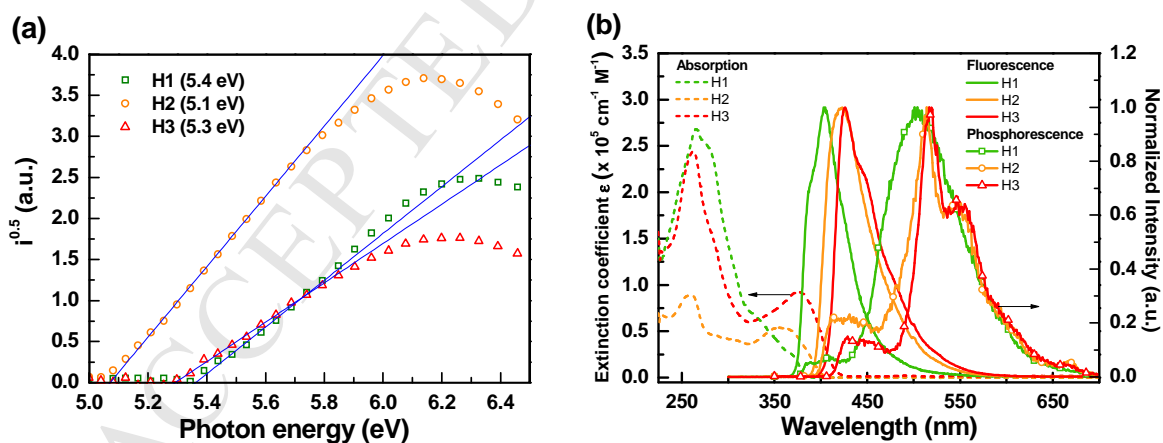


Figure 3 (a) electron photoemission spectra of thin layers of materials **H1**, **H2**, and **H3**; (b) absorption spectra, fluorescence spectra, and phosphorescence spectra of the compounds in dichloromethane.

Figure 3(b) shows the UV-vis absorption spectra and the photoluminescence (PL) spectra of the fabricated materials dissolved in dichloromethane recorded at 300K and 77 K. The PL spectra measured at 77K aimed to characterize the triplet energy of the compounds. In the UV-vis absorption spectra, each material exhibits a peak at around 260 nm, which is related to the absorption bands of the imidazole moiety in the three compounds [21]. Notably, absorption peaks appear at around 360 nm in **H2** and **H3** whereas no peak appears for **H1**, indicating that the absorption bands should originate from the triphenylamine moiety [22]. On the other hand, **H1** exhibits respectively a highest-energy fluorescence and phosphorescence peaks at around 404 nm and 504 nm. Comparing the molecular structure of **H1**, an extension of conjugation length design was introduced in the **H2** and **H3** molecules. The fluorescence (and phosphorescence) peaks of **H2** and **H3** were respectively red-shifted to 423 nm (514 nm) and 426 nm (517 nm). Furthermore, both **H2** and **H3** possess similar spectral profiles demonstrating that the additional imidazole moiety in **H3** doesn't significantly affect its photophysical properties. The triplet energy gap of each material was higher than those found in orange or red phosphors, thus enabling their use as host materials in red PhOLEDs applications. The corresponding photophysical and thermal properties are summarized in Table 1.

Table 1. Photophysical and thermal properties of compounds **H1**, **H2** and **H3**.

	$\lambda_{\text{abs}}^{\text{a}}$ (nm)	$\lambda_{\text{fluo}}^{\text{b}}$ (nm)	$\lambda_{\text{phos}}^{\text{c}}$ (nm)	E_{g}^{d} (eV)	E_{T}^{e} (eV)	I_{p}^{f} (eV)	T_{g}^{g} (°C)	T_{d}^{h} (°C)
H1	265, 279, 332, 367	404	504	3.22	2.46	5.4		386
H2	258, 359	423	514	3.08	2.41	5.1		414
H3	263, 283, 376	426	517	2.97	2.40	5.3	184	448

^a λ_{abs} : absorption maxima in CH_2Cl_2 . ^b λ_{fluo} : emission maxima of fluorescence in CH_2Cl_2 . ^c λ_{phos} : emission maxima of phosphorescence in CH_2Cl_2 at 77 K. ^d Calculated from the absorption onset. ^e Estimated from the peak of phosphorescence spectrum. ^f Estimated from the electron photoemission spectra. ^g Determined by DSC. ^h Analysed using TGA (5% weight loss).

Red phosphorescent OLEDs with different host materials

Considering the triplet energy gaps of compounds **H1**, **H2** and **H3** (i.e. 2.65 eV, 2.54 eV and 2.46 eV), we attempted to fabricate red phosphorescent OLEDs with a simplified trilayer architecture and investigate their EL characteristics. Generally speaking, a host material should possess a triplet energy gap higher than that of the guest to ensure sufficient energy transfer as well as exciton confinement [23]. Furthermore, the emission of the host material and the absorption spectrum of the guest should have an adequate spectral overlap for iso-energetic transitions. In this study, a highly efficient red phosphor, bis(2-methyldibenzo[*f,h*]quinoxaline) (acetylacetonate) iridium (III), [Ir(MDQ)₂acac], was chosen as the emitter because of its high quantum yield and adequate energy bandgap [24]. On the other hand, to evaluate the performance of the fabricated materials, three commercially available host materials suitable for red-emitting guests were used for comparison, including 2,6-dicarbazo-1,5-pyridine (PYD-2Cz), 4,4',4''-tris(carbazol-9-yl)triphenylamine (TCTA), and 4,4'-bis(*N*-carbazolyl)-1,1'-biphenyl (CBP) [25, 26, 27]. Figure 4 shows the absorption spectrum of Ir(MDQ)₂acac and the PL spectra of the tested host materials, exhibiting different levels of spectral overlapping. Furthermore, di-[4-(*N,N*-ditolylamino)-phenyl]cyclohexane (TAPC) and 1,3-bis[3,5-di(pyridin-3-yl)phenyl]benzene (BmPyPhB) were respectively selected as the hole-transport and electron-transport layers due to their excellent carrier transport capabilities and adequate energy gaps [28, 29]. The tested device with a tri-layer architecture was configured as ITO/TAPC (40 nm)/ host doped with 2 wt.% of Ir(MDQ)₂acac (30 nm)/ BmPyPhB (40 nm)/ LiF (0.8 nm)/ Al (150 nm), where the LiF and aluminium were respectively used as the electron injection layer and the cathode. The host materials for devices A~E are as follows: PYD-2Cz, TCTA, CBP, **H1**, **H2**, and **H3**. Figure 5(a) shows the chemical structure of the organic molecules used while Figure 5(b) exhibits the energy level diagrams of the tested red PhOLEDs.

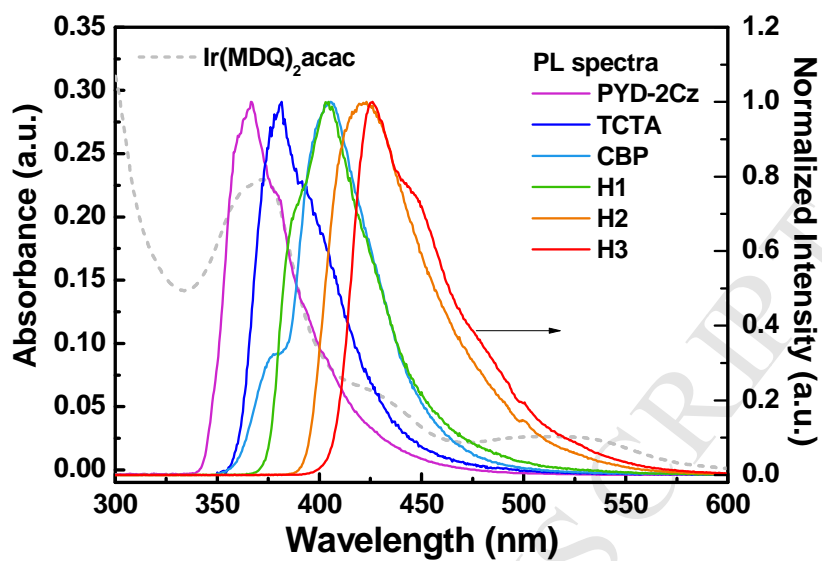


Figure 4. Absorption spectrum of Ir(MDQ)₂acac and PL spectra of the host materials used in this study.

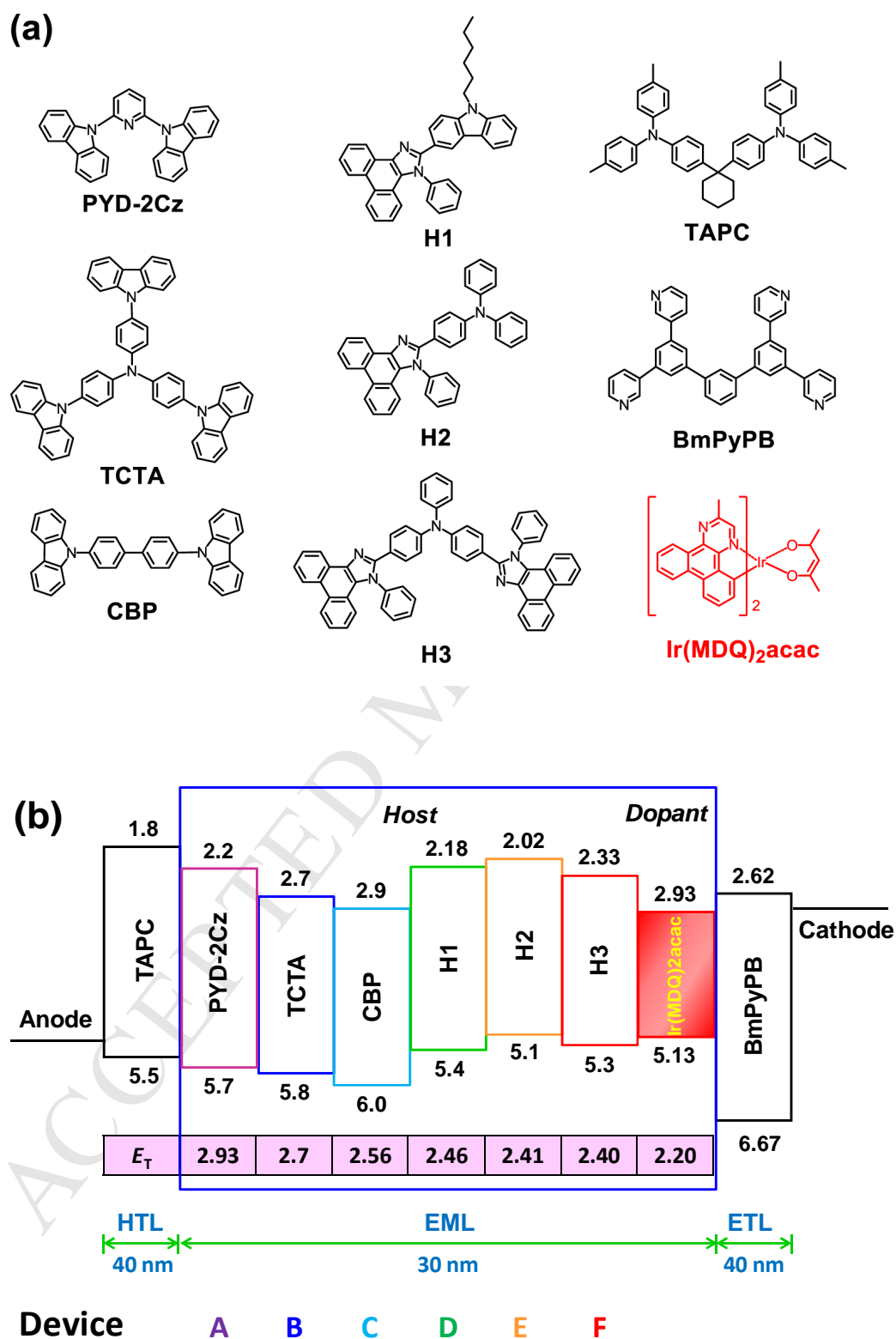


Figure 5. (a) The chemical structure of the used organic materials and (b) energy level diagram of the tested red PhOLEDs.

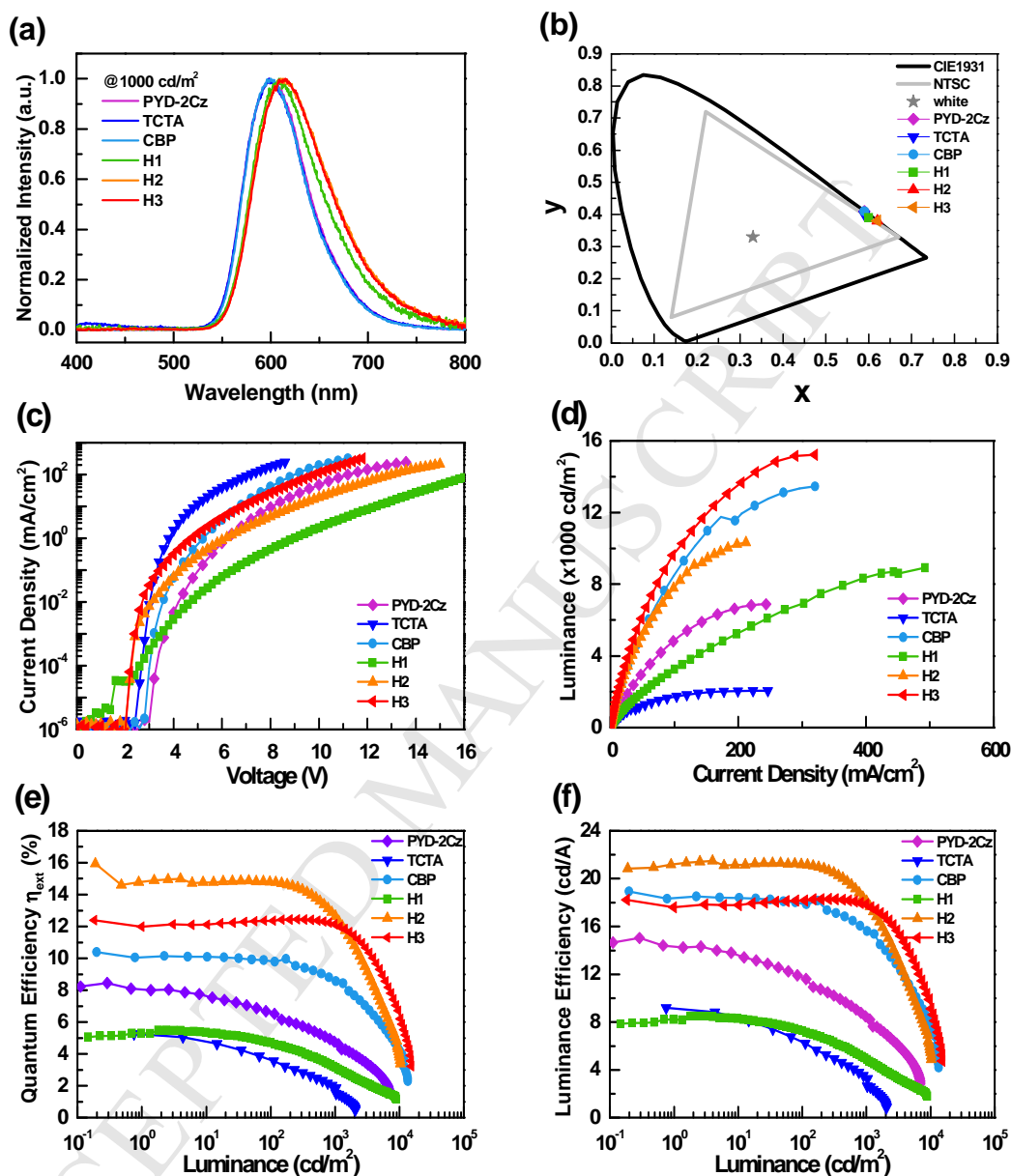


Fig. 6 (a) Normalized EL spectra at a luminance of 10^3 cd/m^2 , (b) CIE coordinates, (c) current density-voltage (J - V) characteristics, (d) luminance-current density (L - J) characteristics, (e) external quantum efficiency versus luminance, and (f) luminance efficiency versus luminance for Devices A (TCTA), B (PYD-2Cz), C (CBP), D (H1), E (H2) and F (H3).

Figure 6 depicts the electroluminescence (EL) characteristics of the PhOLEDs, while the corresponding numeric data are summarized in Table 2. The normalized EL spectra of all devices

recorded at a luminance of 10^3 cd/m² are shown in Fig. 6(a). All devices showed pure Ir(MDQ)₂acac phosphorescence, except for device A, which showed an additional TCTA residual emission, indicating the lack of sufficient doping concentration of the emitter in the TCTA host. Overall, the emission peaks could be clearly divided into two types. The emission peaks for devices with TCTA, PYD-2Cz, and CBP hosts were located at around 600 nm, while devices with fabricated host materials exhibited red-shifted peaks (~611 nm) as well as wider spectral profiles. As indicated, the full width at half maximum (FWHM) of devices using commercially available hosts is about 73 nm, while the devices with compounds **H1**, **H2**, and **H3** possessed rather wider FWHM values (i.e. 82~91 nm). Considering the doping concentration of Ir(MDQ)₂acac, thus molecule stacking could be excluded as the cause of the red-shifted spectra. Instead, the saturated red emissions in devices D~F resulted from the environmental polarity of solid films, making these fabricated compounds more appropriate for use as hosts in red-PhOLEDs with a saturated red emission, thus reducing the difficulty of developing materials for use as red emitters. The CIE coordinates of both the devices E and F were recorded at (0.62, 0.38).

The current-voltage (*J-V*) curves of the tested devices are shown in Fig. 6(b). Comparing the order of the current density recorded at 6V, the sequence of the devices is as follows: TCTA > **H3**~CBP > **H2**~PYD-2Cz > **H1**. Not only does this result in different energy barriers between HTL/EML and EML/ETL, but also the carrier mobility of the host materials influences device current density. Based on the experimental results, the much lower current density obtained in device D might result from the 9-hexylcarbazole structure hindering the carrier transport [³⁰]. Compounds **H2** and **H3** both possess similar energy levels. Device E with the **H2** host gave a higher current density than device D (**H1**), indicating that replacing the 9-hexylcarbazolyl fragment with the triphenylamine moiety in **H2** improves the carrier transport. Furthermore, based on the molecular structure of compound **H2**, compound **H3** has an additional imidazole moiety, giving it an even higher carrier transport capability. Since the energy bandgaps of **H2** and **H3** are much

lower than those of the other tested hosts, the respective turn on voltages of **H2** and **H3** are as low as 2.8 V and 2.6 V. Moreover, the maximum luminance of device F reached 15000 cd/m², which exceeded that of device C with a bipolar CBP host (~13500 cd/m²).

From the efficiency curves shown in Figures 6(e) and (f), the inferior efficiency of device D was attributed to the poor carrier transport ability of **H1**. A similar efficiency was obtained in device A with the TCTA host, but for the opposite reason. Higher hole mobility of the TCTA host resulted in the accumulation of redundant holes in the EML, leading to carrier imbalance. On the other hand, the performance of devices E and F responded very favourably. Devices E and F exhibited EL efficiencies peak of up to 15.9% (21.5 cd/A and 29.9 lm/W) and 12.4% (18.3 cd/A and 23.9 lm/W), respectively. These results indicate that the gradually improved carrier transport capabilities for **H2** and **H3** could result in devices easily achieving carrier balance in a simplified tri-layer architecture. In addition, although the spectral overlap between Ir(MDQ)₂acac and **H2** (or **H3**) is rather low as compared to that of the other hosts, there was no need to raise the doping concentration to achieve effective exothermic energy transfer. In contrast, device C with the commonly used bipolar CBP host only produced a peak external quantum efficiency (EQE) of 10.4%, which is much lower than that of devices E or F. Furthermore, the respective EQEs of devices E and F recorded at 100 (and 1000) cd/m² remained as high as 14.8% (12.7%) and 12.4% (12.1%). Closer inspection of the roll-off behaviour of the tested devices showed the estimated values of external quantum efficiency declined by half at current densities ($J_{1/2}$) of 9.2, 19.4, 73.6, 36.8, 37.6 and 112.7 mA/cm², respectively, for devices A, B, C, D, E and F, respectively [31]. The mitigated efficiency roll-off behaviour observed in device F implies the existence of a diluted exciton concentration in space without serious carrier accumulations at the HTL/EML and EML/ETL interfaces. [32, 33] The adequate energy levels of **H3** enable abundant carrier injection into the EML and thus enlarge the exciton formation zone, simultaneously decreasing the triplet-triplet annihilation and polaron quenching.

Table 2. EL characteristics of tested devices with different host materials.

Device	A	B	C	D	E	F
Host	TCTA	PYD-2Cz	CBP	H1	H2	H3
External [a]	5.3	8.5	10.4	5.5	15.9	12.4
Quantum [b]	3.6	6.6	9.8	4.7	14.8	12.4
Efficiency (%) [c]	1.9	4.7	8.6	3.2	12.7	12.1
Luminescence [a]	9.2	15.0	18.9	8.5	21.5	18.3
Efficiency [b]	6.4	11.7	17.9	7.3	21.2	18.2
(cd/A) [c]	3.3	8.4	15.7	4.9	18.1	17.8
Power [a]	9.6	12.8	18.6	6.5	29.9	23.9
Efficiency [b]	5.1	6.0	11.5	2.4	12.3	13.2
(lm/W) [c]	1.8	3.2	7.7	1.1	7.0	9.0
V_{on} (V) [d]	3.0	4.1	3.4	4.8	2.8	2.6
$J_{1/2}$ (mA/cm ²)	9.2	19.4	73.6	36.8	37.6	112.7
Max. Luminance	2056	6879	13451	8914	10319	15207
(cd/m ²) [Voltage]	[8.6]	[13.6]	[11.2]	[19.8]	[15.0]	[11.8]
$\lambda_{max.}$ (nm)	598	599	600	609	611	613
CIE1931 [b]	(0.59, 0.40)	(0.59, 0.41)	(0.59, 0.41)	(0.60, 0.39)	(0.62, 0.38)	(0.62, 0.38)
coordinates [c]	(0.58, 0.40)	(0.59, 0.41)	(0.59, 0.41)	(0.60, 0.40)	(0.62, 0.38)	(0.62, 0.38)

[a] Maximum efficiency; [b] recorded at 10² cd/m²; [c] measured at 10³ cd/m²; [d] turn-on voltage measured at 1 cd/m².

In summary, the synthesis and full characterization of three newly developed bipolar phenanthro[9,10-*d*]imidazole based derivatives were reported. All the developed compounds and three commercially available derivatives were used as host materials in bis(2-methyldibenzo[*f,h*]quinoxaline) (acetylacetonate) iridium (III) based phosphorescent red organic light emitting diodes. The results indicated that some devices with the newly-developed materials exhibited superior performances to devices using commercial host materials. For comparison, devices with commercial 4,4',4''-tris(carbazol-9-yl)triphenylamine and novel 2-[4-(*N,N*-diphenylamino)phenyl]-1-phenylphenanthro[9,10-*d*]imidazole as the host showed peak efficiencies of 5.3% (9.2 cd/A and 9.6 lm/W) and 15.9% (21.5 cd/A and 29.9 lm/W), respectively. Efficiency of device containing new host material is about 67% higher than those of device containing the commercial host materials.

Acknowledgements

Prof. C.-H. Chang gratefully acknowledge financial support from the Ministry of Science and Technology of Taiwan. (NSC 102-2221-E-155-080-MY3). The OLED materials were developed in the frame of project funded by a grant No. APP-1/2016 from the Research Council of Lithuania. Dr. D. Volyniuk is acknowledged for measurements of ionization potentials.

References

-
- [1] M. A. Baldo, D. F. O'Brien, Y. You, A. Shoustikov, S. Sibley, M. E. Thompson, S. R. Forrest, *Nature* 395 (1998) 151-154.
 - [2] C.-H. Chang, Y.-S. Ding, P.-W. Hsieh, C.-P. Chang, W.-C. Lin, H.-H. Chang, *Thin Solid Films* 519 (2011) 7992-7997.
 - [3] X. Liu, B. Yao, Z. Zhang, X. Zhao, B. Zhang, W.-Y. Wong, Y. Cheng, Z. Xie, *J. Mater. Chem. C*

4 (2016) 5787-5794.

[4] S. Wang, X. Wang, B. Yao, B. Zhang, J. Ding, Z. Xie et al., *Scientific Reports*. 5 (2015) article number 12487.

[5] X. Liu, S. Wang, B. Yao, B. Zhang, C.-L. Ho, W.-Y. Wong, et al., *Org. Electron*. 21 (2015) 1-8.

[6] M.-S. Lin, L.-C. Chi, H.-W. Chang, Y.-H. Huang, K.-C. Tien, C.-C. Chen, C.-H. Chang, C.-C. Wu, A. Chaskar, S.-H. Chou, H.-C. Ting, K.-T. Wong, Y.-H. Liu, Y. Chi, *J. Mater. Chem.* 22 (2012) 870-876.

[7] V. Vaitkeviciene, A. Kruzinauskiene, S. Grigalevicius, J.V. Grazulevicius, R. Rutkaite, V. Jankauskas, *Synthetic Metals*, 158 (2008) 383-390.

[8] K. Chen, H.-R. Zhao, Z.K. Fan, G. Yin, Q.M. Chen, Y.W. Quan, S.H. Ye, *Organic Letters*, 17 (2015) 1413-1416.

[9] S.A. Bagnich, S. Athanasopoulos, A. Rudnick, P. Schroegel, I. Bauer, N.C. Greenham, P. Stroehriegel, *Journal of Physical Chemistry C*, 119 (2015) 2380-2387.

[10] D. Sun, Z. Yang, X. Sun, H. Li, Z.J. Ren, J.T. Liu, D.G. Ma, S.K. Yan, *Polymer Chemistry*, 17 (2014) 5046-5052.

[11] M. Kirkus, J.V. Grazulevicius, S. Grigalevicius, R. Gu, W. Dehaen, V. Jankauskas, *European Polymer Journal*, 45 (2009) 410-417.

[12] M.-H. Tsai, Y.-H. Hong, C.-H. Chang, H.-C. Su, C.-C. Wu, A. Matoliukstyte, J. Simokaitiene, S. Grigalevicius, J. V. Grazulevicius, C.-P. Hsu, *Adv. Mater.* 19 (2007) 862-866.

[13] C.-H. Chang, M.-C. Kuo, W.-C. Lin, Y.-T. Chen, K.-T. Wong, E. Mondal, R. C. Kwong, S. Xia, T. Nakagawa, C. Adachi, *J. Mater. Chem.* 22 (2012) 3832-3838.

[14] J.H. Jou, S. Sahoo, S. Kumar, H.H. Yu, P. H. Fang, M. Singh, G. Krucaite, D. Volyniuk, S. Grigalevicius, J.V. Grazulevicius, *J. Mater. Chem. C*, 3 (2015) 12297-12307.

[15] H.T. Chang, K.Ch. Chiang, F.F. Wong, M.Y. Yeh, *Heterocycles*, 68 (2006) 1585-1594.

[16] A. Vilsmeier, A. Haack, *Chemische Berichte* 60 (1927) 119-123.

- [17] D. Gudeika, A. Michaleviciute, J.V. Grazulevicius, R. Lygaitis, S. Grigalevicius, V. Jankauskas, et al. *J. Phys. Chem. C* 116 (2012) 14811–14819.
- [18] J. Ostrauskaite, V. Voska, J. Antulis, V. Gaidelis, V. Jankauskas, J.V. Grazulevicius, *Journal of Materials Chemistry*, 12 (2002) 3469-3474.
- [19] E. Zaleckas, R. Griniene, B. Stulpinaite, J.V. Grazulevicius, L. Liu, Z. Xie, E. Schab-Balcerzak, E. Kamarauskas, B. Zhang, S. Grigalevicius, *Dyes and Pigments*, 108 (2014) 121-125.
- [20] N.A. Kukhta, D. Volyniuk, L. Peciulyte, J. Ostrauskaite, G. Juska, J.V. Grazulevicius, *Dyes and Pigments*, 117 (2015) 122-132.
- [21] Y. Oyama, H. Kumaoka, K. Uwada, K. Yoshida, *Tetrahedron*, 65 (2009) 8336-8343.
- [22] R. M. F. Batista, S. P. G. Costa, M. M. M. Raposo, *J. Org. Chem.*, 78 (2013) 11389-11395.
- [23] C.-H. Chang, C.-L. Ho, Y.-S. Chang, I.-C. Lien, C.-H. Lin, Y.-W. Yang, J.-L. Liao, Y. Chi, *J. Mater. Chem. C*, 1 (2013) 2639-2647.
- [24] G. Schwartz, S. Reineke, T. C. Rosenow, K. Walzer, K. Leo, *Adv. Funct. Mater.*, 19 (2009) 1319-1333.
- [25] K. S. Son, M. Yahiro, T. Imai, H. Yoshizaki, C. Adachi, *Chem. Mater.*, 20 (2008) 4439-4446.
- [26] G. He, M. Pfeiffer, K. Leo, M. Hofmann, J. Birnstock, R. Pudzich, J. Salbeck, *Appl. Phys. Lett.*, 85 (2004) 3911-3913.
- [27] D. F. O'Brien, M. A. Baldo, M. E. Thompson, S. R. Forrest, *Appl. Phys. Lett.*, 74 (1999) 442-444.
- [28] Y. Zheng, S.-H. Eom, N. Chopra, J. Lee, F. So, J. Xue, *Appl. Phys. Lett.*, 92 (2008) 223301.
- [29] S.-J. Su, E. Gonmori, H. Sasabe, J. Kido, *Adv. Mater.*, 20 (2008) 4189-4194.
- [30] D. Curiel, M. Más-Montoya, C.-H. Chang, P.-Y. Chen, C.-W. Tai, A. Tarraga, *J. Mater. Chem. C*, 1 (2013) 3421-3429.
- [31] H. Sasabe, J. I. Takamatsu, T. Motoyama, S. Watanabe, G. Wagenblast, N. Langer, O. Molt, E. Fuchs, C. Lennartz, J. Kido, *Adv. Mater.*, 22 (2010) 5003-5007.

[32] M. A. Baldo, S. R. Forrest, Phys. Rev. B, 62 (2000) 10967-10977.

[33] D. Hertel, K. Meerholz, J. Phys. Chem. B, 111 (2007) 12075-12080.

ACCEPTED MANUSCRIPT

Bipolar phenanthro[9,10-*d*]imidazole -based compounds have been synthesized and characterized. The compounds are efficient host materials for phosphorescent OLEDs. A red device with efficiency of 15.9% (21.5 cd/A and 29.9 lm/W) was demonstrated.

ACCEPTED MANUSCRIPT